Check for updates

Confluence of montmorillonite and *Rhizobium* towards the adsorption of chromium(VI) from aqueous medium

T. Sathvika,[a] Akhil Raj Kumar Saraswathi,[a] Vidya Rajesh[b] and N. Rajesh [ID] *[a]

Chromium in its hexavalent oxidation state is carcinogenic and wastewater from the electroplating industry is one of the principal sources of pollution. To reduce this toxicity and pave way towards environmental safety, a combination of environmental microbiology and chemistry is quite efficient for developing biosorbents to sequester chromium from waste water. Immobilization of *Rhizobium* in sodium montmorillonite provides a conducive environment to capture hexavalent chromium. Various characterization techniques such as FTIR, XPS and SEM-EDAX were performed and batch parameters such as pH variation, adsorbent dosage, concentration of metal ion and temperature were optimized. Pseudo second order kinetics coupled with a higher regression coefficient for Freundlich isotherm and a Langmuir adsorption capacity of 22.22 mg g^{-1} was achieved for the adsorption process. The adsorption was enhanced by the charge interactions between the protonated clay-*Rhizobium* surface and Cr(VI) ions in acidic medium. The biosorbent was stable and easily regenerated using NaOH. Preliminary column studies were performed to test the efficiency of the developed biosorbent at higher volumes on a laboratory scale.

1. Introduction

Heavy metal contamination is a major issue and is mainly caused by anthropogenic activities. Chromium is regarded as one of the toxic heavy metals. The principal sources for chromium discharge encompass the tanning, leather, cement and electroplating industries. Even though chromium exists in various oxidation states ranging from −2 to +6, the stable oxidation states are +3 and +6 respectively.[1] Trace amounts of trivalent chromium is useful in regulating lipid and glucose metabolism and also it is less mobile compared to its hexavalent form. Due to its high mobility the hexavalent form is highly toxic, entering the cell and interfering with the functioning of proteins, lipids and DNA by producing reactive oxygen species (ROS).[2,3] Hence, USEPA has categorized stipulated hexavalent chromium under group A carcinogen and the chromium permissible limit in drinking water is less than 0.1 mg L^{-1}.[4] Therefore, development of various remediation methods for chromium is necessary. Several physico-chemical techniques such as reverse osmosis, adsorption, precipitation, chemical coagulation, ion exchange are used in the treatment of chromium contaminated waste water. However, some of the processes are not cost effective and have shortcomings such as sludge generation, use of higher volumes

of reagents and greater energy consumption.[5] In order to combat most of these disadvantages, biosorption has proven to be a viable choice for the removal and recovery of heavy metals.

The surface adsorption process which involves the use of active or inactive microbes is termed as biosorption. When the active microbes are involved in adsorption it is termed to be active mechanism and is a metabolism dependent process, wherein use of inactive microbes is metabolism independent passive mechanism.[6] There are also some drawbacks with the direct use of primitive microbes such as poor mechanical strength, regeneration ability and microbial separation from solvent.[7] Hence immobilization of microbes in suitable matrices helps in gaining porosity, rigidity, mechanical strength, low sludge formation, easy handling and good regeneration ability.[8] The functional groups present in the microbial cell walls aid in complexing the heavy metals.[9] The bio based and eco-friendly materials are used for many applications. Recent literature highlights the importance of bio based materials and eco-friendly sorbents. The utility of molecularly imprinted biopolymers based on a green synthesis strategy for determination of B-family vitamins[10] and for clean separation of baclofen from bio-fluid samples has been reported.[11] Molecularly imprinted nanoparticles based on functionalized silica as an efficient sorbent for the determination of acrylamide in potato chips and a green synthetic route for water-compatible molecularly imprinted nanoparticles for the extraction of hydrochlorothiazide from human urine has been reported recently.[12,13]

The removal of Cr(VI) by few of the recently reported biosorbents include *Saccharomyces cerevisiae* immobilized in crosslinked

[a]Department of Chemistry, Birla Institute of Technology and Science, Pilani-Hyderabad Campus, Hyderabad 500 078, India. E-mail: nrajesh05@gmail.com; Fax: +91 40 66303998; Tel: +91 40 66303503

[b]Department of Biological Sciences, Birla Institute of Technology and Science, Pilani-Hyderabad Campus, Hyderabad 500 078, India

cellulose using microwave radiation has an adsorption capacity of 23.61 mg g^{-1}.[14] The immobilization of *Rhizobium* and yeast in functionalized carbon nanotubes have Langmuir adsorption capacities of 24.86 mg g^{-1} and 31.6 mg g^{-1} for Cr(VI) removal.[15] *Aspergillus* BVR immobilized in sodium montmorillonite[16] and cellulose[17] also showed good efficacy in adsorbing Cr(VI). Adsorption coupled reduction of Cr(VI) has been observed as the mechanism involving the inactive biomass of *Aspergillus niger*.[18]

The nitrogen fixing bacteria *Rhizobium* is a Gram negative, rod shaped prokaryote which provides nutrients to the plants by increasing the agronomic output and also helps in regulating fungal root infections.[19,20] The carbon and nitrogen sources available in the sludge generated from the agro based industries offers an economic route for growth of *Rhizobium* and also a sustainable alternative in wastewater treatment.[21] Cr(III) at pH 7.0 was removed using the activated biomass of *Rhizobium leguminosarum* with an efficiency of 84.4 ± 3.6%.[22] Clays possess hydrous aluminosilicate tetrahedral and octahedral layers with cation exchange properties and has several advantages such as large surface area, ordered structure, intercalation and good thermal and chemical stabilities.[23] Montmorillonite is a 2 : 1 type of clay with an aluminum tetrahedron sheet sandwiched between two silica octahedral sheets with exchangeable cations which counteract the negative charge produced in the isomorphic substitution.[24] There are several reports on adsorption of Cr(VI) using clays such as montmorillonite supported magnetite nanoparticles that could adsorb up to 15.3 mg g^{-1} Cr(VI). Clay–biopolymer composites such as cellulose-clay[25] also has good potential for Cr(VI) removal. The reduction of Cr(VI) has been correlated to the content of Fe^{2+} ions present in dithionite reduced smectite.[26]

As the microbe-clay combination can exist in similar ecological environment it could remove several organic pollutants.[27] Hence the combination of inactive or dead microbes in conjunction with clays would be advantageous to sequester hexavalent chromium. There are relatively few reports for heavy metal sequestration using microbial–clay combination. The current study demonstrates and highlights the importance of microbe modified sodium montmorillonite for Cr(VI) removal wherein the isolated *Rhizobium* species was immobilized in clay using ultrasonication. The developed clay-*Rhizobium* biosorbent was subjected to comprehensive characterization and batch studies were conducted to adsorb Cr(VI) from aqueous medium.

2. Materials and methods

2.1. Chemicals and materials

Analytical and guaranteed grade reagents were used throughout the experiments. A 1000 mg L^{-1} Cr(VI) stock solution was prepared using K$_2$Cr$_2$O$_7$ (Merck) and various working concentrations were prepared by further dilution. Ultrapure (Millipore) water was used to prepare aqueous solutions. Montmorillonite, K-10 was purchased from Sigma Aldrich. The chemicals used in the YMA (Yeast extract, Mannitol) media for microbial culture were procured from Himedia, India.

An ultra-sonication bath (Biotechnics, India) was used for the immobilization of *Rhizobium* BVR in montmorillonite. Various analytical techniques were used to characterize the developed

biosorbent. FTIR spectrum was recorded using JASCO-4200 model FTIR spectrometer by mixing 100 mg of KBr with 1 mg of the biosorbent. A S3400N model Scanning electron microscope (Hitachi) which was associated with Thermo Electron EDAX system was used to understand the morphology of the biosorbent. A post derivatized technique for the estimation of Cr(VI) at 540 nm after the adsorption was performed using 883 Basic IC plus Ion chromatography with UV-Visible detector. Leica DMi8 laser scanning confocal microscopy (S/N 418513) with a TCS SP8 scanner was used to obtain the confocal images. A Jasco V650 UV visible spectrophotometer was used to determine the concentration of chromium(VI) during the column studies. The survey scan spectra was recorded using XPS PHI 5000 Versa Prob II, FEI Inc, using aluminum monochromator of power 25.4 W and 187.8 eV.

2.2. Preparation of the clay-*Rhizobium* biosorbent

The sodium form of montmorillonite (NaMMT) was prepared by treating montmorillonite with sodium chloride as described in literature.[28] The isolated *Rhizobium* BVR was grown in YMA broth medium and complete characterization of the microbe has been reported in our earlier studies[15] and assigned an accession number MF136764 by NCBI genbank. The grown culture was centrifuged to obtain a pellet. A 2.0 g weight of *Rhizobium* was mixed with 1.0 g of NaMMT in aqueous medium and subjected to sonication for about 8 min (50 W, 230 V) to ensure the bacterial surface immobilization in sodium montmorillonite. The NaMMT-*Rhizobium* biosorbent was filtered, rinsed with water and dried for further experimental studies. The biosorbent developed is pale yellow in color and has varied functional groups which could adsorb Cr(VI).

2.3. Synthesis of probes for Cr(VI) and Cr(III)

Cr(VI) and Cr(III) were also differentiated by specific binding probes such as Rhodamine sensors where the spirolactam structure and spiro ring opening mechanism play a key role. The synthesis of Cr species specific probes, Rhodamine B hydrazide (RBH)[29] and Rhodamine based chemosensor (RF)[30] was done as described previously. The probes synthesized were mixed with the samples for capturing the laser confocal microscopy images.

2.4. Biosorption studies

The biosorption experiments were optimized by conducting batch studies using 0.2 g of the prepared NaMMT-*Rhizobium* biosorbent in 30 mL of 5 mg L^{-1} working Cr(VI) solution. The temperature variations at different time intervals with an agitation speed of 120 rpm was performed in an incubator shaker (Biotechnics, India). The Cr(VI) concentration left in solution was quantitatively analyzed using ion chromatography technique through post column derivatization using diphenyl carbazide.[31] The adsorption capacity of the biosorbent containing Cr(VI) (mg g^{-1}) after reaching equilibrium (q_e) was calculated using

$$q_e = \frac{(C_o - C_e)V}{W} \tag{1}$$

where q_e = Cr(VI) (mg g^{-1}) after adsorption onto biosorbent, C_o = initial Cr(VI) concentration (mg L^{-1}), C_e = Cr(VI) concentration
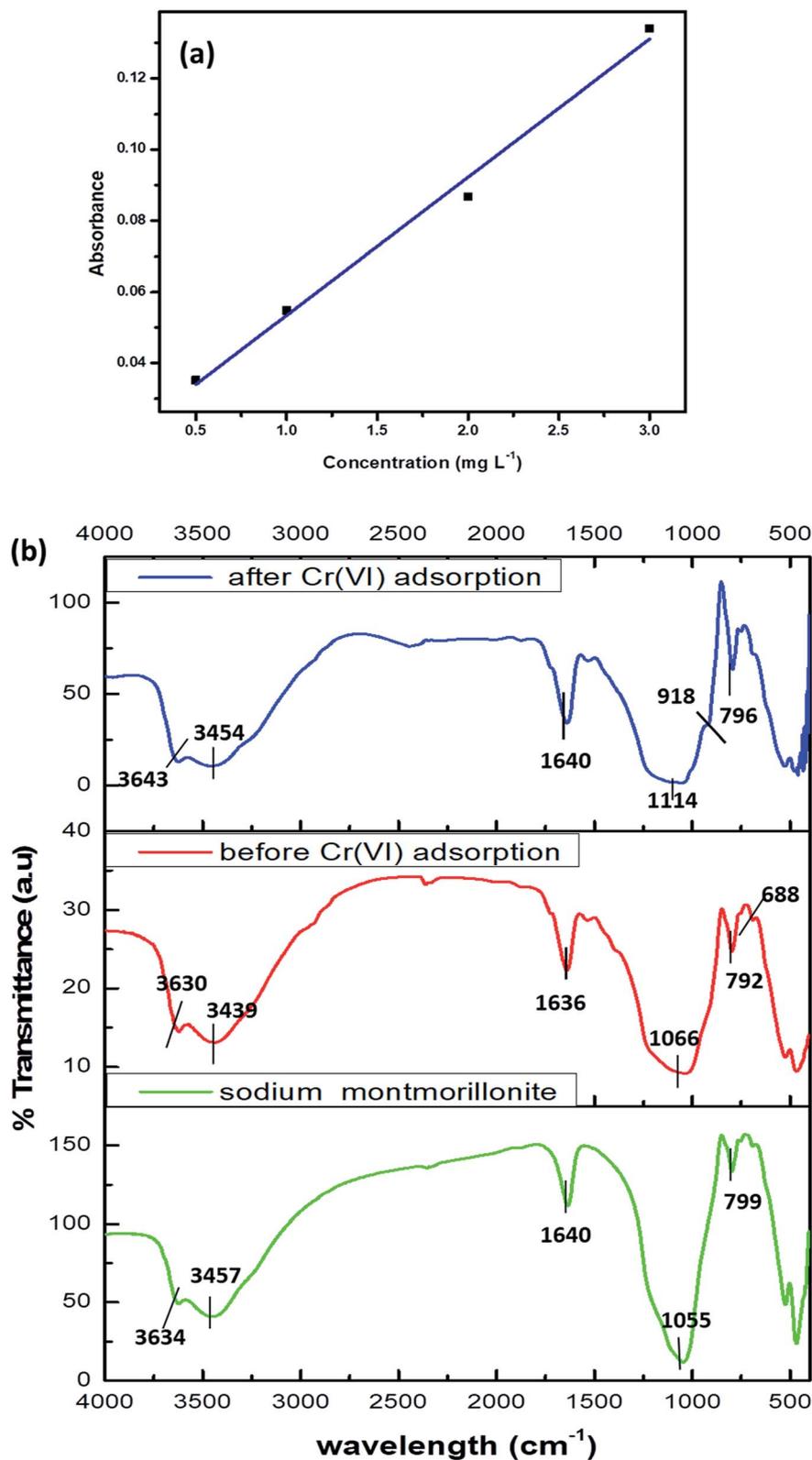
Fig. 1 (a) Calibration graph of Cr(VI) (b) FTIR of sodium montmorillonite, biosorbent before and after Cr(VI) adsorption.

at equilibrium (mg L^{-1}) V = volume of Cr(VI) solution (L) and W = weight of clay-*Rhizobium* biosorbent (g).

The calibration graph of Cr(VI) was performed in the range 0–3 mg L^{-1} and is presented in Fig. 1a.

3. Results and discussion

3.1. Characterization of the clay-*Rhizobium* biosorbent

The frequency shifts in the IR spectrum reveals the participation of hydroxyl, amino, carboxyl functional groups present in the microbial cell walls. The characteristic band for clays was observed at 3643 cm^{-1} corresponding to the Si–OH functional groups.[16,32] The hydroxyl and amine functional groups and also the Al–O–H stretching vibrations together contribute to the broad band at 3454 cm^{-1}. The Si–O–Si stretching of clay was observed at 1114 cm^{-1} and the amide-I band at 1640 cm^{-1} (ref. 32) could be attributed to the bacteria and hydrogen bonding in water. The other characteristic peaks for montmorillonite at 792 cm^{-1} and 688 cm^{-1} indicates the broadening of quartz and silica and Si–O bond deformation respectively.[25] A shouldering peak at 918 cm^{-1} corresponding to Cr=O after adsorption of hexavalent chromium[16] is an evidence for metal adsorption as shown in Fig. 1b.

The morphological features of the *Rhizobium* immobilized in clay captured using SEM showed assorted clusters (Fig. 2) and also the elemental analysis through EDAX showed the presence of elements such as Na, K, Al, Si respectively. The presence of Cr

peak between 5–6 keV after adsorption confirmed Cr(VI) adsorption (Fig. 2). The possible reduction of Cr(VI) was explored using X-ray photo electron spectroscopy since microbial adsorption mechanism is often coupled with reduction. The survey scan revealed the presence of elements such as C, O, N, Cr (Fig. 3a) and the short scan of the C 1s peak was corrected to 284.8 eV (Fig. 3b). The binding energies in the survey scan showed a peak at 576.9 eV that corresponds to Cr(III) and 585.7 eV which is characteristic of Cr(VI).[33] It was observed that there was no immediate reduction after biosorption of Cr(VI) and the clay-*Rhizobium* surface turned pale green only after few days signifying the formation of Cr(III).

Specific rhodamine based sensors were utilized in the characterization to differentiate Cr(III) and Cr(VI) with laser confocal microscopy by using probes such as RBH and RF as discussed in our earlier work.[15,29,30] The bright field and fluorescent images are shown in Fig. 4a–h. The images captured before and after addition of probes confirmed the presence of Cr(VI) and Cr(III) respectively. The pink color formation indicates the presence of chromium in their respective oxidation states using the above probes.

3.2. Effect of pH, adsorbent dosage and interaction mechanism for biosorption

In accordance with the pH of the aqueous phase, hexavalent chromium is present as hydrogen chromate (HCrO$_4^-$),

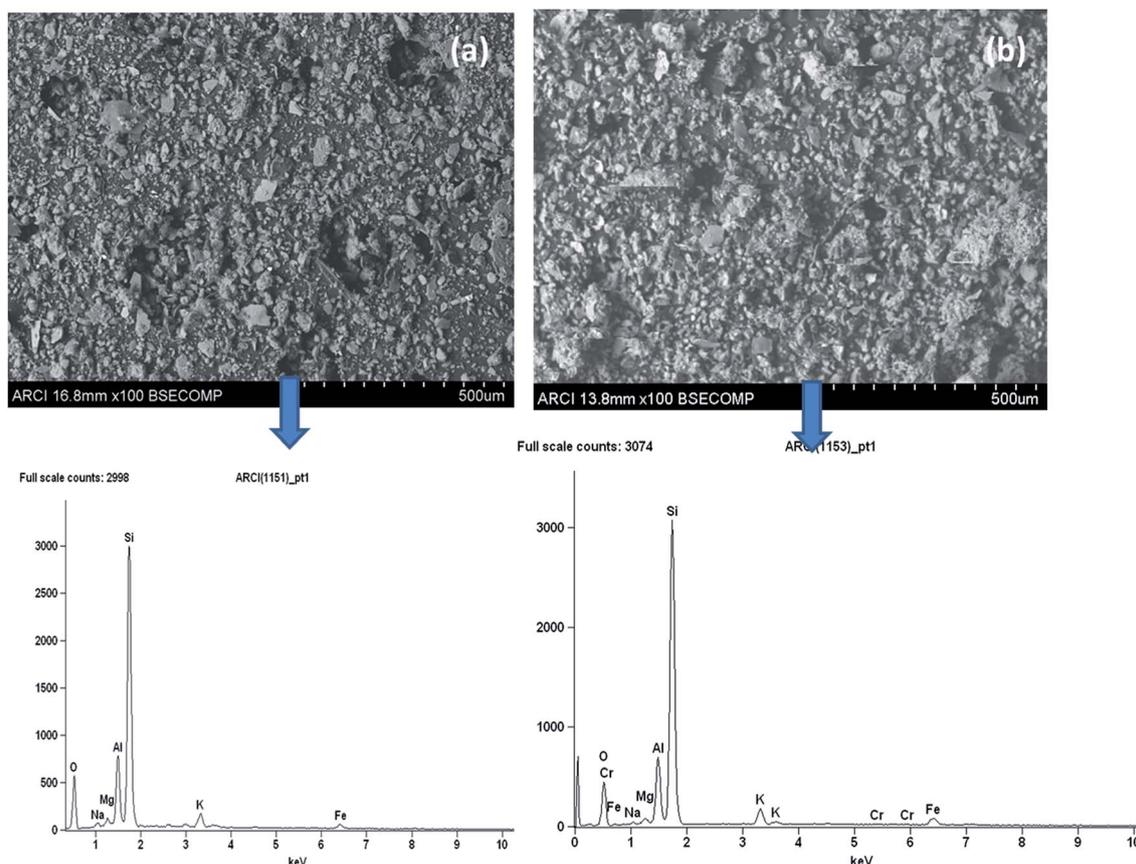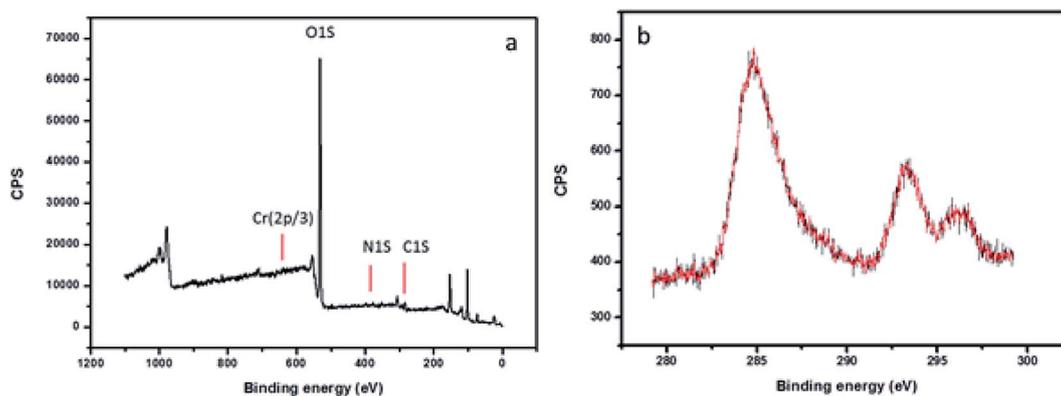Fig. 2 SEM and EDAX images of the biosorbent (a) before Cr(VI) adsorption (b) after Cr(VI) adsorption.

Fig. 3 XPS spectra of the biosorbent after Cr(VI) adsorption (a) survey scan spectra (b) high resolution spectra of C 1s.

dichromate ($Cr_2O_7^{2-}$) and chromate (CrO_4^{2-}) oxy anions respectively. The dichromate and hydrogen chromate anions exist in equilibrium and the plausible mechanism indicates the existence of $HCrO_4^-$ at pH greater than or equal to 2.0.[34] Quantitative adsorption was observed on the surface of the biosorbent at pH 2.0 for a 30 mL volume of 5 mg L^{-1} hexavalent chromium concentration (Fig. 5a). The functional groups such as amine, carboxyl, hydroxyl (from microbial surface), silanol and aluminol groups (from clay) are protonated at pH 2.0 resulting in electrostatic interactions with hydro chromate ions.[16,25] According to hard–soft acid base concept, Cr(VI) in the form of hydrochromate anion reacts with protonated nitrogen and oxygenated functional groups of the biosorbent resulting in electrostatic interactions.[25] At pH 2.0 and at a adsorbent dosage of 0.2 g, 30 mL of 5 mg L^{-1} Cr(VI) was adsorbed completely beyond which saturation of active binding sites was observed (Fig. 5b). With increase in pH, decline in adsorption was

observed due to the deprotonation of functional groups present on the surface of clay-*Rhizobium* biosorbent.

3.3. Equilibrium adsorption isotherms, kinetics and thermodynamic studies

The association between the adsorbent and the adsorbate at equilibrium was studied using isotherms.[35] The data obtained (Table 1) is very useful in understanding the mechanism and was fitted with classical isotherms.[36] The data obtained (Fig. 6a–d) depicts the increase in adsorption at higher Cr(VI) concentrations gradually leading to saturation. The Langmuir model assumes monolayer sorption in which metal ion adsorption occurs on a homogenized surface and there is no contact between the adsorbed ions. The multilayer adsorption which occurs on a heterogeneous surface is described by Freundlich model. Among the two models, Freundlich isotherm, with r^2
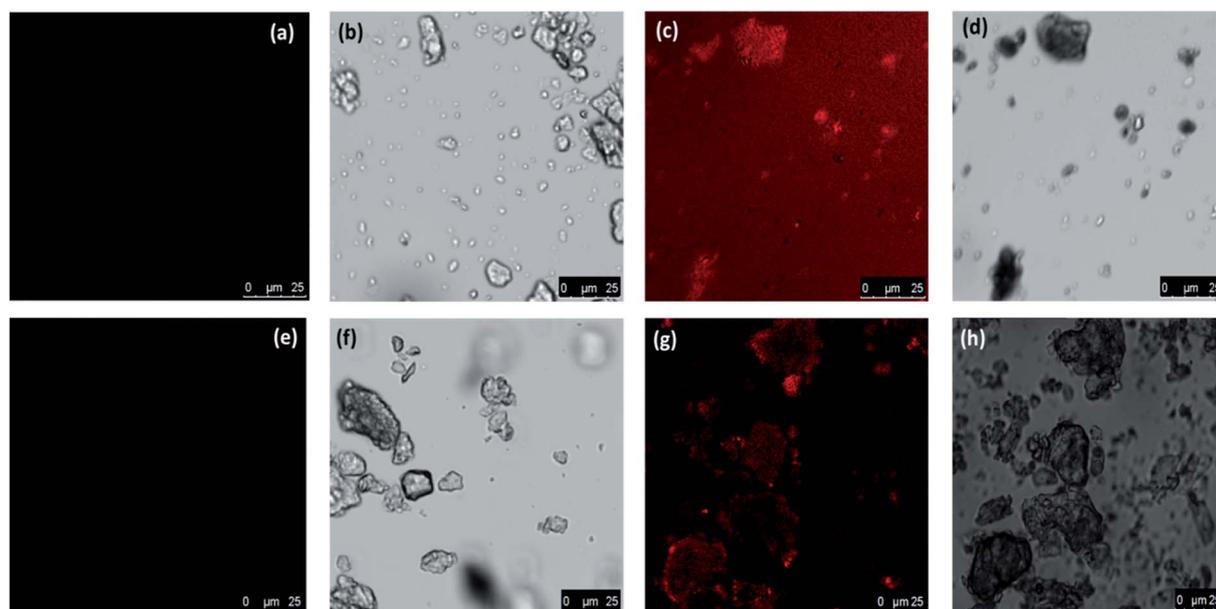

Fig. 4 Confocal using laser source and bright field images of the biosorbent after Cr(VI) adsorption (a and b) without RBH (c and d) with RBH (e and f) without RF (g and h) with RF.
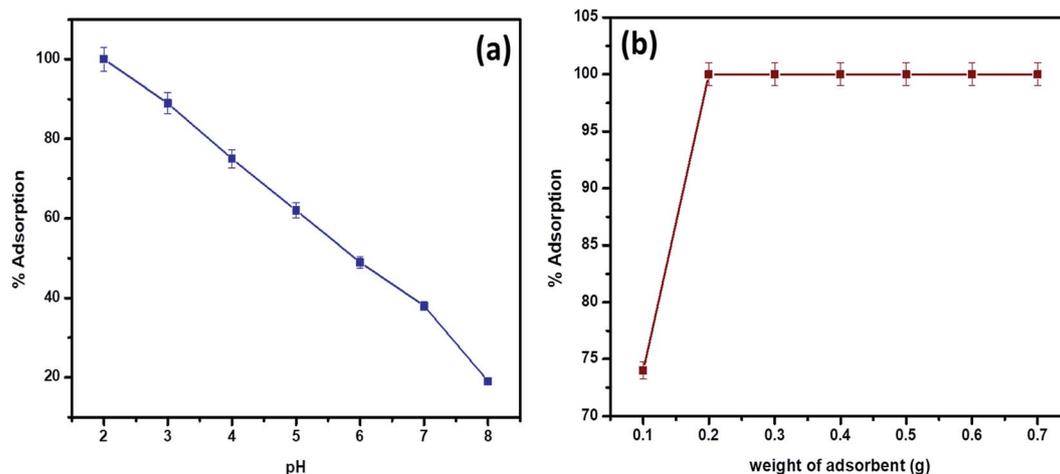
Fig. 5 (a) pH effect on biosorption (at 30 °C, 5 mg L^{-1} Cr(vi)) (b) variation of adsorbent dosage (at pH 2.0, 30 °C, 5 mg L^{-1} Cr(vi)).

value of 0.99 and a low χ^2 value of 0.03 was quite appropriate in describing the adsorption process. The favorability of adsorption is also indicated by the value of the exponent in which lies in range of 1–10. The Langmuir adsorption capacity of the system was found to be 22.22 mg g^{-1} with 0.93 as correlation coefficient and R_L (a dimensionless parameter) given as $R_L = 1/1 + bC_o$,[37] was below unity and this confirmed the suitability and reversibility of adsorption. *Rhizobium* BVR strain as such could adsorb Cr(vi) with an adsorption capacity of 11.5 mg g^{-1}. In addition, Temkin and Dubinin Radushkevich (D–R) isotherms were also studied through the respective plots (Fig. 6) and the corresponding parameters are given in Table 1. Temkin isotherm assumes that there is a linear decrease in the enthalpy of adsorption with incremental surface coverage by the adsorbate. The mean energy obtained from the D–R isotherm which is less than 8 kJ mol^{-1} indicates that the physical adsorption process involves the electrostatic interaction between the functional groups on the *Rhizobium*-clay surface and hexavalent chromium. The low r^2 values obtained with Temkin and D–R isotherms indicates that the adsorption mechanism could only be best described through Langmuir and Freundlich isotherms. The maximum adsorption capacities of various related adsorbents[15,25,38–41] reported in literature are given in Table 2.

The kinetics of the Cr(vi) adsorption was assessed for varying contact time period ranging from 5 min to 180 min. An adsorption efficacy of 60% was achieved during initial five minutes and later the adsorption rate continued to raise steadily and attained equilibrium at 180 min. The adsorption kinetics were evaluated using the pseudo first order[42] and second order kinetics[43] equations as shown below

$$\log(q_e - q_t) = \log q_e - \frac{k_1 t}{2.303}$$

$$\frac{t}{q_t} = \frac{1}{k_2 q_e^2} + \frac{t}{q_t}$$

A working solution of 10 mg L^{-1} Cr(vi) was used for the kinetic studies. The data obtained from the kinetic plots (Fig. 6e and f) are tabulated in Table 3. The system followed pseudo second order kinetics with observed and calculated q_e values as 1.0446 and 1.020 mg g^{-1}. The Cr(vi) uptake is majorly driven by the mechanisms such as film, particle diffusion and surface adsorption. At high Cr(vi) concentrations, intraparticle diffusion plays a major role whereas at low metal concentrations pore diffusion takes place.[14] The boundary layer mechanism for efficient metal uptake is well explained by Weber–Morris intra particle diffusion model and was obtained by plotting q_t and $\sqrt{t}$ (Fig. 6g) and ascertained through the non-zero intercept.

Table 1 Langmuir, Freundlich, Temkin and D–R isotherm parameters

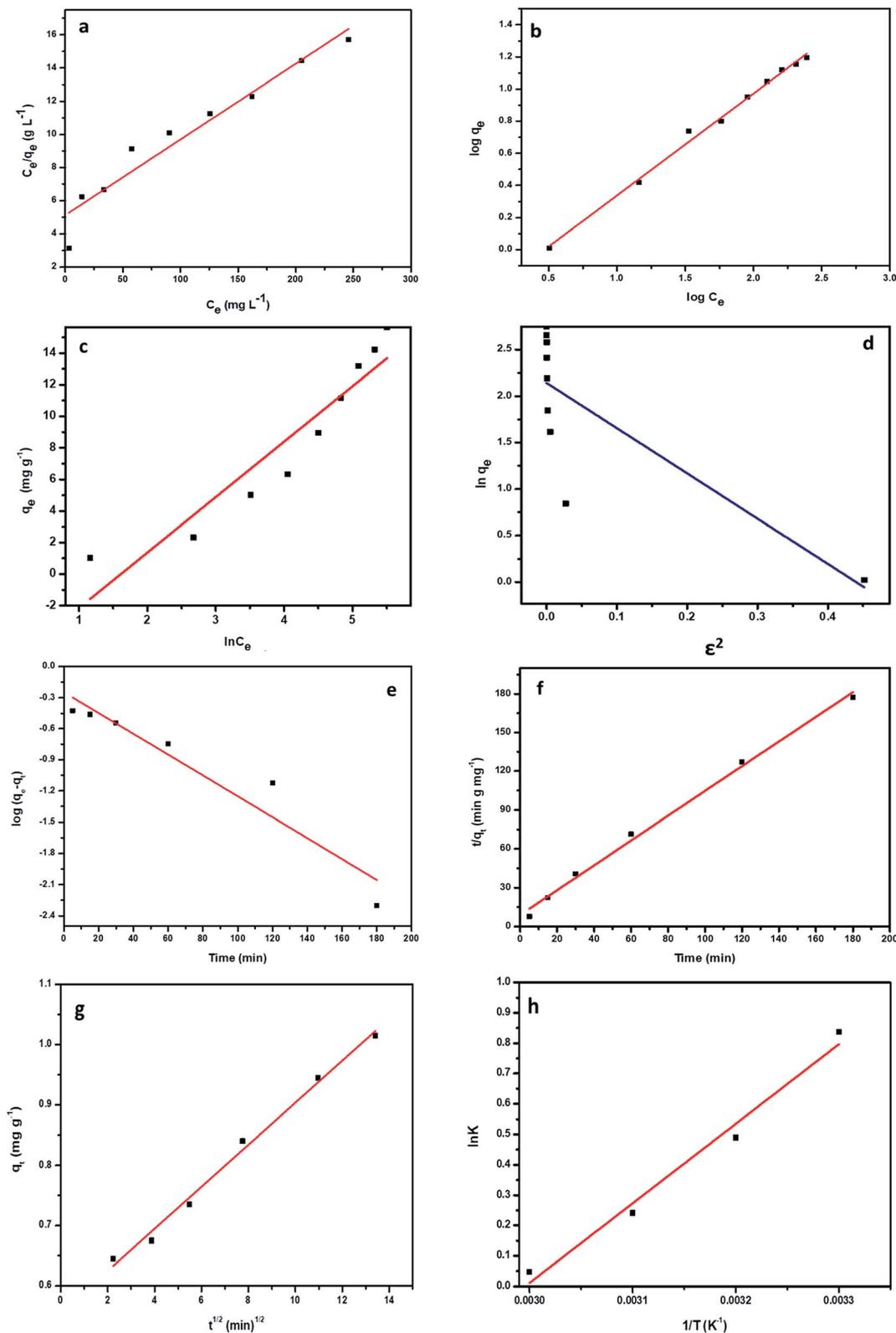|					
Langmuir, $\frac{C_e}{q_e} = \frac{1}{q_o b} + \frac{C_e}{q_o}$	q_o (mg g^{-1}), 22.22	b (L mg^{-1}), 0.0087	R_L, 0.9199	r^2, 0.9315	χ^2, 0.0685
Freundlich, $\log q_e = \log K_F - \frac{1}{n}\log C_e$	K_F (mg$^{1-1/n}$ g^{-1} L$^{1/n}$), 0.5058	n, 1.5755	—	r^2, 0.9935	χ^2, 0.0386
Temkin, $q_e = \frac{RT}{b}\ln K_T + \frac{RT}{b}\ln C_e$, $B = RT/b$	K_T (L g^{-1}), 0.199	B (J mol^{-1}), 3.512	—	r^2, 0.876	
Dubinin Radushkevich (D–R), $\ln q_e = \ln q_m - \beta\varepsilon$, $E = \frac{1}{\sqrt{-2\beta}}$	q_m (mg g^{-1}), 8.519	β (mol^2 kJ^{-2}), 4.86	E (kJ mol^{-1}), 0.32	r^2, 0.56	

Fig. 6 (a) Langmuir isotherm (b) Freundlich isotherm (c) Temkin isotherm (d) D–R isotherm (e) plot of pseudo first order kinetics (f) plot of pseudo second order kinetics (g) intra particle diffusion (h) Van't Hoff plot.

The changes in the thermodynamic parameters such as enthalpy (ΔH), Gibbs free energy (ΔG), and entropy (ΔS) at various temperatures signifies the feasibility and nature of the adsorption reaction. The transfer of chromium from solution phase occurs onto the immobilized bacterial cell surface wherein montmorillonite acts as the primary host and the clay–

Table 2 Comparison of biosorption capacities against few related adsorbents

Adsorbents	pH	Biosorption capacity (mg g^{-1})
Cellulose-sodium montmorillonite[25]	3.8–5.5	22.2
Magnetic nanoparticles[38]	6.0	3.0
Montmorillonite supported nanoparticles[39]	4.0	15.3
Bacterial cellulose[40]	1.5	5.13
Bacillus marisflavi[41]	5.0	5.78
(Present study)	2.0	
Only *Rhizobium* BVR		11.5
Only Na montmorillonite		9.51
Rhizobium BVR immobilized in sodium montmorillonite		22.22

Table 3 Kinetic parameters associated with biosorption

| C_o (mg L^{-1})	q_e (mg g^{-1})	k_2 (g mg^{-1} min^{-1})	R^2	k_1 (min^{-1})	R_1^2	k_{int} (mg g^{-1} min$^{-0.5}$)
10	1.0446	0.0584	0.9943	0.0231	0.9031	0.034

bacteria biosorbent acts as a secondary host for Cr(VI). The overall reaction Gibb's free energy change (ΔG_r) can be explained as a summation from clay-*Rhizobium* surface and clay-*Rhizobium*-chromium surface.

$$\Delta G_r = \Delta G_{\text{clay-}Rhizobium\text{ surface}} + \Delta G_{\text{clay-}Rhizobium\text{-Cr}}$$

The reaction Gibb's free energy can also be correlated to the enthalpy and entropy changes as

$$\Delta G_r = \Delta H_{\text{clay-}Rhizobium\text{-Cr}} - T\Delta S_{\text{clay-}Rhizobium\text{-Cr}}$$

At equilibrium,

$$\text{Clay-}Rhizobium\text{-Cr}_{\text{(solution)}} \rightleftharpoons \text{clay-}Rhizobium\text{-Cr}_{\text{(surface)}}$$
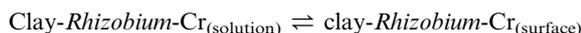
$$\Delta G_r = \Delta G_r^0 + RT \ln \frac{a_{\text{[clay-}Rhizobium\text{-Cr]}_{\text{surface}}}}{a_{\text{[clay-}Rhizobium\text{-Cr]}_{\text{solution}}}}$$

The chemical potential $\mu_{\text{Cr}} = \mu_{\text{Cr}}^0 + RT \ln a_{\text{Cr (solution)}}$

In dilute solutions at ppm levels, it is reasonable to approximate the activity, $a = c$.

Therefore,

$$\Delta G_r = \Delta G_r^0 + RT \ln \frac{\text{[clay-}Rhizobium\text{-Cr]}_{\text{surface}}}{\text{[clay-}Rhizobium\text{-Cr]}_{\text{solution}}}$$

Hence,

$$\Delta G_r = \Delta G_r^0 + RT \ln K_c$$

At equilibrium $\Delta G_r = 0$.

$$\Delta G_r^0 = -RT \ln K_{\text{eq}}$$

From the plot of ln K against $1/T$ (Fig. 6h) the thermodynamic parameters namely, enthalpy and entropy changes were obtained from slope and intercept (Table 4). The biosorption process was spontaneous as observed from negative free energy values. Further, from the negative values of enthalpy, it is obvious that adsorption reaction is exothermic. The range of ΔH (20–40 kJ mol^{-1}) also indicates physico–chemical adsorption phenomenon.[15] The negative ΔS value is attributed to the decreased randomness at the clay-*Rhizobium*-aqueous interface.

3.4. Column studies

3.4.1. Effect of sample volume. A higher volume of metal ion solution was tested with the developed biosorbent by performing small scale column studies. A 2.0 g of biosorbent was packed in a glass column of 30 cm length and 2 cm width up to a bed height of 3 cm (Fig. 7a). A 50 mL volume of 5 mg L^{-1} Cr(VI) was passed through the column continuously and assessed periodically (10 mL portions) for the presence of Cr(VI) using UV-

Table 4 Thermodynamic parameters involved in the biosorption

Temperature (Kelvin)	$\Delta G°$ (kJ mol^{-1})	$\Delta S°$ (J mol^{-1} K^{-1})	$\Delta H°$ (kJ mol^{-1})
303	−2.11	−65.202	−21.765
313	−1.273		
323	−0.646		
333	−0.132		
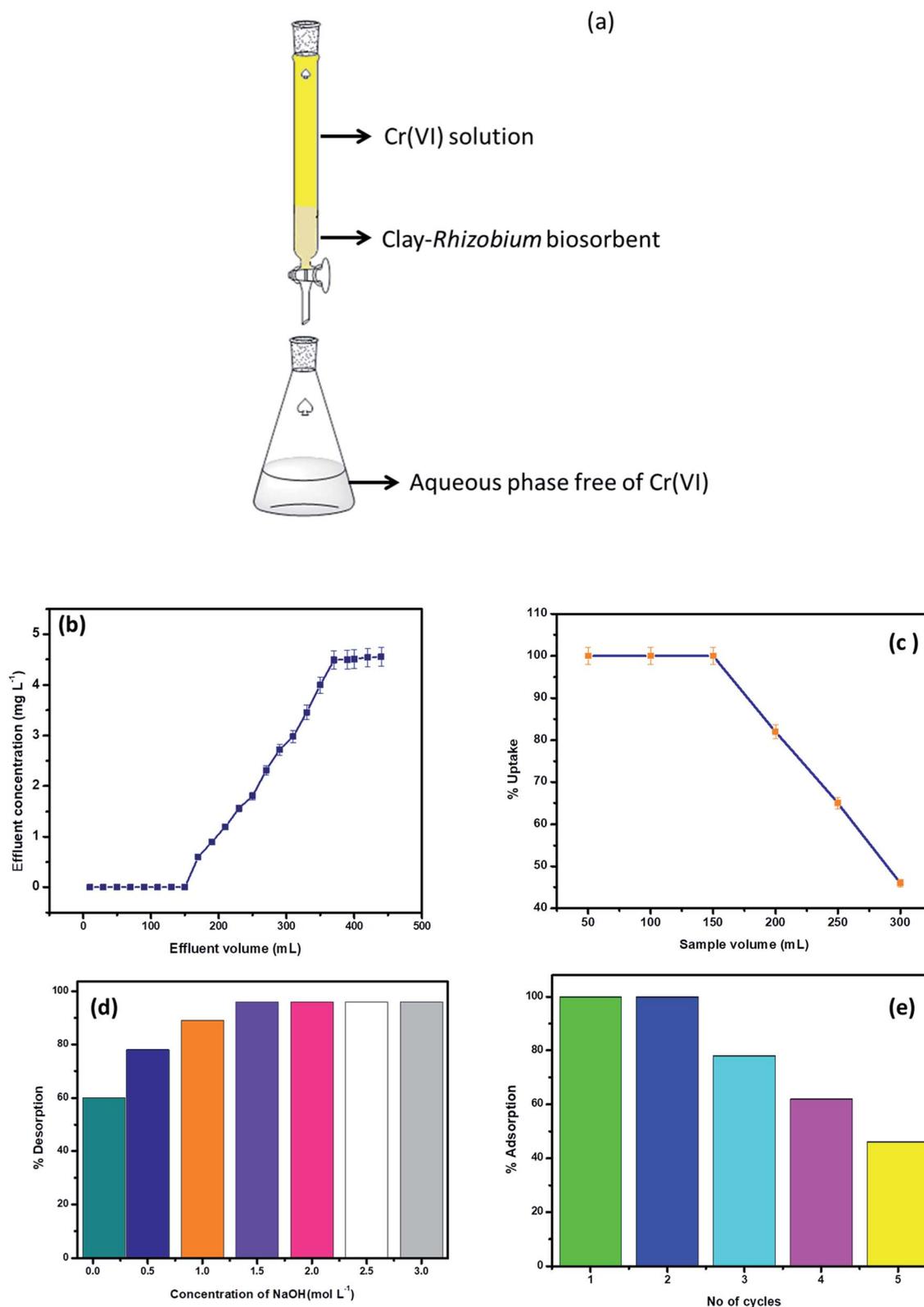
Fig. 7 (a) Diagrammatic representation of column setup for Cr(vi) treatment (b) breakthrough curve (c) effect of sample volume (d) effect of varied NaOH concentrations (e) regeneration efficiency of the biosorbent.

visible spectrophotometry with diphenyl carbazide as the complexing agent.[16] A sample volume of 150 mL could be treated quantitatively beyond which the saturation of active adsorption sites decreased the metal ion adsorption (Fig. 7b and c). At higher volumes, the swelling of clay results in expansion of the bed and reduces the adsorption efficiency.

3.4.2. Regeneration of the clay-*Rhizobium* biosorbent and application studies. The reusability of clay-*Rhizobium* biosorbent was tested using desorbing agents that were selected carefully not to inflict any damage to the biosorbent surface. The Cr(VI) adsorbed onto the biosorbent surface was eluted as sodium chromate using 10 mL of 1.5 mol L^{-1} NaOH[15,44] (Fig. 7d). Quantitative adsorption of chromium was achieved in the first two cycles and in the third cycle the adsorption was 78%, followed by 62% and 46% in the fourth and fifth cycles respectively (Fig. 7e). Repeated adsorption–desorption cycles under alkaline conditions would deprotonate the biosorbent surface resulting in reduction of active sites of the biosorbent surface. The eluted Cr(VI) was converted to Cr(III) (less toxic) and diluted to ppb levels to minimize direct disposal of higher levels of hexavalent chromium.

The effect of diverse ionic constituents were studied independently as well as in a mixture in the concentration range as reported earlier.[15,17] Accordingly, the interference studies were performed by preparing a synthetic mixture containing ions such as Cu^{2+}, Pb^{2+}, Co^{2+}, Ni^{2+}, Fe^2, nitrate, chloride and sulphate at 100 mg L^{-1} level using 5 mg L^{-1} Cr(VI) solution. Due to the interference of sulphate and Fe^{2+}, reduction in Cr(VI) adsorption was observed and the formation of stable metal chloro complexes [$CoCl_4{}^{2-}$, $NiCl_4{}^{2-}$] also compete with hydrochromate ions thereby lowering the percentage adsorption of hexavalent chromium from aqueous phase.[15]

4. Conclusions

The developed clay-*Rhizobium* biosorbent showed good efficacy in adsorbing Cr(VI) from liquid phase. The adsorption followed pseudo second order kinetics and equilibrium is attained in 180 min with a Langmuir adsorption capacity of 22.22 mg g^{-1}. Protonated surface functional groups on the *Rhizobium* cell surface and montmorillonite promotes effective interaction with the hydrochromate ions from liquid phase. The thermodynamics of adsorption was observed to be less random, exothermic, and spontaneous with negative entropy ($\Delta S° = -65.202$ J mol^{-1} K^{-1}), enthalpy ($\Delta H° = -21.765$ kJ mol^{-1}) and free energy changes. The presence of Cr(VI) and trace Cr(III) were confirmed by XPS and confocal microscopy. The regeneration of biosorbent using NaOH was effective up to two cycles from a sample volume of 150 mL was also validated in a synthetic mixture of diverse ions at 100 mg L^{-1} concentration.

Conflicts of interest

The authors declare no competing interests.

Acknowledgements

References

1 K. Choi, S. Lee, J. O. Park, J. A. Park, S. H. Cho, S. Y. Lee, J. H. Lee and J. W. Choi, Chromium removal from aqueous solution by a PEI-silica nanocomposite, *Sci. Rep.*, 2018, **8**, 1438.

2 J. F. Gutierrez-Corona, P. Romo-Rodríguez, F. Santos-Escobar, A. E. Espino-Saldana and H. Hernández-Escoto, Microbial interactions with chromium: basic biological processes and applications in environmental biotechnology, *World J. Microbiol. Biotechnol.*, 2016, **32**, 191.

3 A. S. K. Kumar, S. J. Jiang and W. L. Tseng, Effective adsorption of chromium(VI)/Cr(III) from aqueous solution using ionic liquid functionalized multiwalled carbon nanotubes as a super sorbent, *J. Mater. Chem. A*, 2015, **3**, 7044–7057.

4 USEPA, *Analytical feasibility document for the six year review of existing national primary drinking water regulation, office of ground water and drinking water EPA 815R 03*, EPA, Washington DC, 2003.

5 B. Dhal, H. N. Thatoi, N. N. Das and B. D. Pandey, Chemical and microbial remediation of hexavalent chromium from contaminated soil and mining/metallurgical solid waste: a review, *J. Hazard. Mater.*, 2013, **250–251**, 272–291.

6 M. Fomina and G. M. Gadd, Biosorption: current perspectives on concept, definition and application, *Bioresour. Technol.*, 2014, **160**, 3–14.

7 J. R. Dodson, H. L. Parker, A. M. García, A. Hicken, K. Asemave, T. J. Farmer, H. V. He, J. H. Clark and A. J. Hunt, Bio-derived materials as a green route for precious & critical metal recovery and re-use, *Green Chem.*, 2015, **17**, 1951–1965.

8 M. Shanmugaprakash and V. Sivakumar, Competitive biosorption of Cr(VI) and Zn(II) ions in single and binary-metal systems onto a biodiesel waste residue using batch and fixed-bed column studies, *RSC Adv.*, 2015, **5**, 45817–45826.

9 V. Javanbakht, S. A. Alavi and H. Zilouei, Mechanisms of heavy metal removal using microorganisms as biosorbent, *Water Sci. Technol.*, 2014, **69**, 1775–1787.

10 A. Ostovan, M. Ghaedi, M. Arabi, Q. Yang, J. Li and L. Chen, Hydrophilic Multi-template Molecularly Imprinted Biopolymers Based on a Green Synthesis Strategy for Determination of B-family Vitamins, *ACS Appl. Mater. Interfaces*, 2018, **10**, 4140–4150.

11 A. Ostovan, M. Ghaedi and M. Arabi, Fabrication of water-compatible superparamagnetic molecularly imprinted biopolymer for clean separation of baclofen from bio-fluid samples: a mild and green approach, *Talanta*, 2018, **179**, 760–768.

12 M. Arabi, A. Ostovan, M. Ghaedi and M. K. Purkait, Novel strategy for synthesis of magnetic dummy molecularly imprinted nanoparticles based on functionalized silica as an efficient sorbent for the determination of acrylamide in

potato chips: optimization by experimental design methodology, *Talanta*, 2016, **154**, 526–532.

13 M. Arabi, M. Ghaedi and A. Ostovan, Development of a Lower Toxic Approach Based on Green Synthesis of Water-Compatible Molecularly Imprinted Nanoparticles for the Extraction of Hydrochlorothiazide from Human Urine, *ACS Sustainable Chem. Eng.*, 2017, **5**, 3775–3785.

14 T. Sathvika, Manasi, V. Rajesh and N. Rajesh, Microwave assisted immobilization of yeast in cellulose biopolymer as a green adsorbent for the sequestration of chromium, *Chem. Eng. J.*, 2015, **279**, 38–46.

15 T. Sathvika, A. Soni, K. Sharma, M. Praneeth, M. Manasi, V. Rajesh and N. Rajesh, Potential application of *Saccharomyces cerevisiae* and *Rhizobium* immobilized in multiwalled carbon nanotubes to adsorb hexavalent chromium, *Sci. Rep.*, 2018, **8**, 9862.

16 T. Sathvika, Manasi, V. Rajesh and N. Rajesh, Prospective application of *Aspergillus* species immobilized in sodium montmorillonite to remove toxic hexavalent chromium from wastewater, *RSC Adv.*, 2015, **5**, 107031–107044.

17 T. Sathvika, M. Manasi, V. Rajesh and N. Rajesh, Leveraging the Potential of Endomycorrhizal Spores and Montmorillonite for Hexavalent Chromium Adsorption from Aqueous Phase, *ChemistrySelect*, 2018, **3**, 2747–2755.

18 D. Park, Y. S. Yun, J. H. Jo and J. M. Park, Mechanism of hexavalent chromium removal by dead fungal biomass of *Aspergillus niger*, *Water Res.*, 2005, **39**, 533–540.

19 S. Sivakumaran, P. Lockhart and B. D. Jarvis, Identification of soil bacteria expressing a symbiotic plasmid from *Rhizobium leguminosarum* bv. *Trofolii.*, *Can. J. Microbiol.*, 1997, **43**, 164–177.

20 S. Ehteshamul-haque and A. Ghaffar, Use of Rhizobia in the Control of Root Rot Diseases of Sunflower, Okra, Soybean and Mungbean, *J. Phytopathol.*, 1993, **138**, 157–163.

21 F. B. Rebah, D. Prévost, A. Yezza and R. D. Tyagi, Agro-industrial waste materials and wastewater sludge for rhizobial inoculant production: a review, *Bioresour. Technol.*, 2007, **98**, 3535–3546.

22 N. Raaman, B. Mahendran, C. Jaganathan, S. Sukumar and V. Chandrasekaran, Removal of chromium using *Rhizobium leguminosarum*, *World J. Microbiol. Biotechnol.*, 2012, **28**, 627–636.

23 N. García-Gonzalez, B. A. Frontana-Uribe, E. Ordonez-Regil, J. Cardenas and J. A. Morales-Serna, Evaluation of Fe^{3+} fixation into montmorillonite clay and its application in the polymerization of ethylenedioxythiophene, *RSC Adv.*, 2016, **6**, 95879.

24 B. S. Kumar, A. Dhakshinamoorthy and K. Pitchumani, K10 Montmorillonite clays as environmentally benign catalysts for organic reactions, *Catal. Sci. Technol.*, 2014, **4**, 2378–2396.

25 A. S. K. Kumar, S. Kalidhasan, V. Rajesh and N. Rajesh, Application of cellulose-clay composite biosorbent toward the effective adsorption and removal of chromium from industrial wastewater, *Ind. Eng. Chem. Res.*, 2012, **51**, 58–69.

26 R. W. Raylor, J. S. Shen, W. F. Bleam and S.-i tu, Chromate removal by dithionite-reduced clays: evidence from direct X-ray adsorption near edge spectroscopy (XANES) of chromate reduction at clay surfaces, *Clays Clay Miner.*, 2000, **48**, 648–654.

27 H. Dong, Clay–Microbe Interactions and implications for environmental mitigation, *Elements*, 2012, **8**, 113–118.

28 M. Boufait and H. A. Amar, Removal of *N,N*-dimethylaniline from a dilute aqueous solution by Na^+/K^+ saturated montmorillonite, *Desalination*, 2007, **206**, 300–310.

29 Y. Xiang, L. Mei, N. Li and A. Tong, Sensitive and selective spectrofluorimetric determination of chromium(VI) in water by fluorescence enhancement, *Anal. Chim. Acta.*, 2007, **581**, 132–136.

30 Y. Zhou, J. Zhang, L. Zhang, Q. Zhang, T. Ma and J. Niu, A rhodamine-based fluorescent enhancement chemosensor for the detection of Cr^{3+} in aqueous media, *Dyes Pigm.*, 2013, **97**, 148–154.

31 E. J. Arar and J. D. Pfaff, Determination of dissolved hexavalent chromium in industrial wastewater effluents by ion chromatography and post-column derivatization with diphenylcarbazide, *J. Chromatogr. A*, 1991, **546**, 335–340.

32 D. Naumann, Infra-red spectroscopy in microbiology, *Encyclopaedia of Analytical Chemistry*, ed. R. A. Meyers, John Wiley and Sons Ltd., Chichester, 2000, pp. 102–131.

33 Y. Mu, Z. Ai, L. Zhang and F. Song, Insight into core–shell dependent anoxic Cr(VI) removal with $Fe@Fe_2O_3$ nanowires: indispensable role of surface bound Fe(II), *ACS Appl. Mater. Interfaces*, 2015, **7**, 1997–2005.

34 J. D. Ramsey and R. L. McCreery, *In situ* Raman microscopy of chromate effects on corrosion pits in aluminum alloy, *J. Electrochem. Soc.*, 1999, **146**, 4076–4081.

35 M. Ghanimati, M. Jabbari, A. Farajtabar and S. A. Nabavi-Amri, Adsorption kinetics and isotherms of bioactive antioxidant quercetin onto amino-functionalized silica nanoparticles in aqueous ethanol solutions, *New J. Chem.*, 2017, **41**, 8451.

36 Y. Chen, B. Wang, J. Xin, P. Sun and D. Wu, Adsorption behavior and mechanism of Cr(VI) by modified biochar derived from Enteromorpha prolifera, *Ecotoxicol. Environ. Saf.*, 2018, **164**, 440–447.

37 C. Sun, L. Sun and X. Sun, Graphical evaluation of the favorability of adsorption processes by using conditional Langmuir constant, *Ind. Eng. Chem. Res.*, 2013, **52**, 14251–14260.

38 Y. C. Sharma and V. Srivastava, Comparative studies of removal of Cr(VI) and Ni(II) from aqueous solutions by magnetic nanoparticles, *J. Chem. Eng. Data*, 2011, **56**, 819–825.

39 P. Yuan, M. Fan, D. Yang, H. He, D. Liu, A. Yuan, J. Zhu and T. Chen, Montmorillonite-supported magnetite nanoparticles for the removal of hexavalent chromium [Cr(VI)] from aqueous solutions, *J. Hazard. Mater.*, 2009, **166**, 821–829.

40 M. Lu, Y. Xu, X. Guan and D. Wei, Preliminary research on Cr(VI) removal by bacterial cellulose, *J. Wuhan Univ. Technol., Mater. Sci. Ed.*, 2012, **27**, 572–575.

41 S. Mishra and M. Doble, Novel chromium tolerant microorganisms: isolation, characterization and their

biosorption capacity, *Ecotoxicol. Environ. Saf.*, 2008, **71**, 874–879.

42 A. K. Mishra, V. K. Shahi, N. R. Agrawal and I. Das, Synthesis, characterization, and application of a thiophene–pyrrole copolymer as an efficient adsorbent for removal of methylene blue, *J. Chem. Eng. Data*, 2018, **63**, 3206–3214.

43 Y. S. Ho and G. Mckay, The kinetics of sorption of divalent metal ions onto sphagnum moss peat, *Water Res.*, 2000, **34**, 735–742.

44 T. Sathvika, S. Balaji, M. Chandra, A. Soni, V. Rajesh and N. Rajesh, A co-operative endeavor by nitrifying bacteria *Nitrosomonas* and zirconium based metal organic framework to remove hexavalent chromium, *Chem. Eng. J.*, 2019, **360**, 879–889.